THE UNIVERSITY *of* EDINBURGH

Edinburgh Research Explorer

Underestimated change of wet-bulb temperatures over East and South China

OPEN ACCESS

Underestimated Change of Wet-Bulb Temperatures Over East and South China

N. Freychet[1], S.F.B. Tett[1], Z. Yan[2], and Z. Li[2]

[1]School of Geosciences, University of Edinburgh, Edinburgh, UK, [2]Institute of Atmospheric Physics, University of Chinese Academy of Sciences, Beijing, China

Abstract Wet-bulb temperature (TW), which combines dry-bulb temperature and relative humidity (RH), is a key variable for human health and heat stress because in hot environments evaporation is the main process by which bodies cool down. For this study, we use two independent RH data sets: a new homogenized network of daily ground observations in China and the recent ERA5 reanalysis, for which we highlight the need to apply humidity correction. Based on these data sets, we show that Chinese wet-bulb temperatures since 1980 have increased largely due to a rise in dry-bulb temperatures while RH has remained approximately constant. We also find that TW change has been previously underestimated due to humidity bias in reanalysis and nonhomogenized observation where RH was decreasing sharply after 2000s, greatly limiting changes in TW.

1. Introduction

Heat stress and its impact on human health are often studied through a combined measurement (wet-bulb temperature, TW) of dry-bulb temperature (T) and relative humidity (RH) because in hot environments evaporation is the main process by which bodies cool down (Davis et al., 2016). A TW of 35 °C has been identified as a limit threshold for survivability (Sherwood & Huber, 2010) when the human body cannot cool, leading to heat stroke within a few hours. RH is itself a function of dry-bulb temperature, leading to a complex behavior of wet-bulb temperature. For this study, we use two independent RH data sets: a new homogenized network of daily ground observations in China and the recent ERA5 reanalysis, for which we highlight the need to apply humidity correction. Based on these data sets, we show that Chinese wet-bulb temperatures since 1980 have increased largely due to a rise in dry-bulb temperatures while RH has remained constant. If dry-bulb temperature change have been a leading mechanism, humidity supply over land has also been important, as it allowed TW to increase at the same rate as dry-bulb temperature. We also found that using nonhomogenized RH data sets would lead to greatly underestimating the change in TW. Our results question the potential impact of future humidity constraint (with development of large-scale irrigation for agriculture for example) on TW. Reduction of RH over land could slightly limit the increase in TW while artificial wetting could have opposite effect, leading to amplified increase in TW.

Eastern China and southern China are influenced by the summer monsoon circulation, which brings humid air from the nearby oceans and dry air from the northwesterlies. It also has a complex topography, ranging from a wide low-elevation plain (North China plain) to hilly areas in the South. These features lead to complex humidity and temperature interactions. More than a billion people live in this area, making it a region highly vulnerable to changes in climate.

2. Materials and Methods

Here we present the data used for this study. We also introduce a methodology to remove some inconsistency between data sets (elevation and urbanization effects and correction of RH) for a better comparison. Finally, we present the method to compute TW.

2.1. Data Sets
2.1.1. ERA5 Reanalysis
ERA5 reanalysis (Hersbach et al., 2018) is available for the full satellite observation period (1979 to present). It aims to improve on the ERA-Interim product (Dee et al., 2011). A main improvement is that outputs are provided at hourly time scales at 0.25° resolution on a reduced Gaussian grid, allowing better analysis of
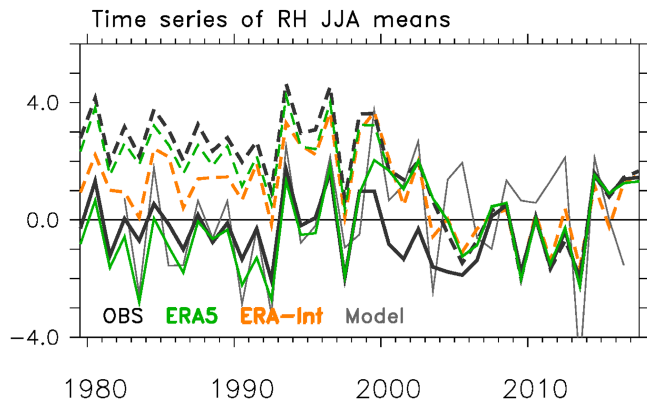
Figure 1. Correction of relative humidity evolution during the 1979–2017 period. JJA mean anomalies of RH (in %) relative to the last decade (2008–2017) over the south and east China region (black boxes in Figure 2b) for ERA5 (masked only where OBS are available) before (dashed green line) and after (solid green line) applying correction, for ERA-Interim (dashed orange line), nudged model experiment (solid gray line), and homogenized OBS (solid black line). Observations from same stations as OBS but without homogenization is also shown with dashed black line.

temporal and spatial variability of climate signals. More information on this data set can also be found online (https://www.ecmwf.int/en/forecasts/datasets/reanalysis-datasets/era5).

2.1.2. Observations

A dense network of 756 station records (OBS; Li & Yan, 2009), provided by the China Meteorological Administration, is used. It provides daily values for mean, minimum and maximum surface temperatures, and daily mean for surface RH. Temperature measurements have been homogenized to remove artifacts due to station relocation or instrument changes (Li & Yan, 2009). We also use a new version of homogenized RH observation as a reference (available to download at http://www.sciencedb.cn/dataSet/handle/804; Li et al., 2020). A part of the inhomogeneities in observation also came from the frequency of measurement to compute the daily values. For manual record, daily values were based on three or four measurements during the day. Since they became automatic, daily values are based on hourly means (thus 24 values per day). This change in sampling frequency explains part of inhomogeneities in nonhomogenized data sets.

To compare more easily with ERA5 reanalysis, OBS is gridded to the same grid as ERA5, by averaging all stations available at each grid cell (and masking points without stations). The grid is complete over much of eastern and southern China but is scarce over central and western China (Figure S1a in the supporting information). OBS records go back to 1950 (although it is considered unreliable before 1960), but to be consistent with ERA5, only the 1979–2017 period is used.

2.2. RH and Bias Correction

To compute wet-bulb temperature (TW) reliable dry-bulb temperatures and RHs are needed. The former has been documented in previous studies (e.g. Li & Yan, 2009; Freychet et al., 2017; Freychet et al., 2018 for observations and ERA-Interim; and supplementary material for ERA5). Observations of RH is traditionally less used in climate studies, as it is rarely homogenized and prone to error (Willett et al., 2008; Willett et al., 2014). Both nonhomogenized observation and reanalysis (ERA Interim and ERA5) show a sharp drop in RH after 2000 (Figure 1). This transition has been identified as an artifact due to change in observation methods, most of the stations switching from manual to automatic recording during early 2000s (Yu & Mou, 2008; Yuan et al., 2010; Zhu et al., 2015). Reanalysis apparently assimilated these biased data. As RH is needed to compute wet-bulb temperature, and to be more consistent with homogenized OBS, we corrected RH in ERA5 before the 2000s. To do so independently from OBS, we use results from a global atmospheric model nudged to ERA-Interim dynamics and using historical sea surface temperature, sea ice concentration, greenhouses concentration, and aerosol emissions (Freychet et al., 2019). Given these settings, it represents observed dynamics at large scales. Although surface humidity in the model is not perfect, it has a good correlation with observations. It does not exhibit any sharp drop after 2000s, confirming RH has remained fairly constant (in the model).

Bias in ERA5 is corrected before 2000 by applying a correction factor so the difference between ERA5 and the model (with a 3-year running mean) should be similar as the 2000–2017 mean difference. Doing so, we managed to cancel the sharp artifact while keeping the variability in ERA5. Note that the correction is only implement during JJA, and it is computed individually at each grid point (as bias vary spatially). Both OBS and corrected ERA5 show no trend in RH during 1979–2017 (Figure 1). We expect trends to be more reliable in corrected ERA5 compared to noncorrected data. Previous studies using ERA-Interim or ERA5 RH over China region should be considered carefully (although the bias in ERA-Interim is definitely weaker, at least for the JJA means).

We also tested the sensitivity of results by applying a correction after 2000s to ERA5 instead of before. Doing so leads to slightly higher TW during the historical period (due to higher RH) but do not change conclusions on trends.

2.3. Computation of Wet-Bulb Temperatures

Wet-bulb temperature (TW) is not provided directly from observational records or reanalysis outputs and needs to be computed. Different approaches are possible, but all need surface air temperature, humidity, and pressure. We use an empirical computation formula (Stull, 2011) that uses atmospheric surface temperature and RH (which contains both humidity and pressure information), both being available for station data sets. The Stull formulation is valid for RH between 5% and 99% and for temperatures from −20 to 50 °C (Stull, 2011), which are reasonable ranges for this study. The empirical formula is also mostly valid at standard sea level pressure. At other pressure levels this formula can slightly underestimate the actual value of TW, especially under very dry conditions (Figure 2 of Stull, 2011). In this study this is not a problem as pressure level is quite homogeneous over South and East China and the region has a relatively high humidity. Results for Western China on the other hand should be considered carefully as pressure level varies greatly in Himalayan region.

Surface humidity is not directly provided by ERA5 (or ERA-Interim) but is computed from dew point temperature and surface pressure (as described in https://confluence.ecmwf.int/display/CKB/ERA+datasets%3A+near-surface+humidity).

For OBS, TW is computed at daily time scale (TW_{mean}). As ERA5 provides hourly outputs, TW is computed first computed at hourly time scale, and then outputs are processed to obtain daily mean (TW_{mean}), minimum (TWN), and maximum (TWX) values. If not stated otherwise, results for TW are based on corrected RH for ERA5 and homogenized observation.

Due to the nonlinearity of TW, results based on daily output are slightly different from results based on averaging hourly outputs (Figure S3). Even if these differences are small, less than 0.3 °C overall, and less than 0.1 °C over in South and East China, it can still explain part of the differences between OBS (based on daily variables) and ERA5 (based on hourly variables).

2.4. Elevation and Urbanization Effects
2.4.1. Elevation Effect

Both OBS and ERA5 are temperatures with different meanings: local measurement for OBS and grid mean for ERA5. Stations are often located near cities in valleys, while reanalysis estimates temperatures consistent with grid cell mean elevation. Thus, differences may exist between the two data sets, especially in complex topography regions, because they do not have the same elevation. To test this, we remove the elevation difference following method described in previous work (Freychet et al., 2018). This is done by, for each station, by computing the elevation difference (dz) between the station and the corresponding grid point of ERA5 and modifying the station temperature by a factor linearly proportional to dz. Hutchinson et al. (2009) showed that T_{mean}, TN, and TX do not vary at the same rate with altitude, and so we use the following coefficients: 6, 4, and 8 K per 1,000 m for T_{mean}, TN, and TX, respectively. TW is then computed based on elevation corrected T_{mean}. RH is also corrected according to elevation difference with the following method, using the hypothesis or near-constant specific humidity in boundary layer. First, specific humidity (q_{obs}) for OBS is computed from T_{mean}, RH, and surface pressure at each station. Then RH is recomputed by combining q_{obs} with the elevation corrected T_{mean} (obtained with previous steps) and the surface pressure from ERA5. Finally, TW is computed using both corrected versions of T_{mean} and RH.

Note that this method is not aimed to correct observations but only to estimate how much of the differences between OBS and ERA5 can be explained by difference in elevation alone. Figures S1 and S2 show results of the elevation correction. After removing the elevation effect, differences between ERA5 and OBS are strongly reduced. This confirms that part of the mean bias in ERA5 is because it represents temperatures at different elevations to OBS. Some differences remain for a few stations, possibly due to local effects not included in ERA5.

2.4.2. Urbanization Effect

Wang et al. (2017) used ERA-Interim reanalysis (which does not include urban tiles) and OBS to estimate the effect of urbanization on temperatures. They found out the main effect is on TN with an increase of +1.7 °C for a 100% urban change. The impact on T_{mean} is more moderate (+0.8 °C) and almost negligible for TX.

ERA5 does not include urban tiles either. To test the sensitivity of TW_{mean} trend to urban effect in this data set, we apply a manual adjustment using from Wang et al. (2017). Urban fractions for 1980 and 2009 on a grid
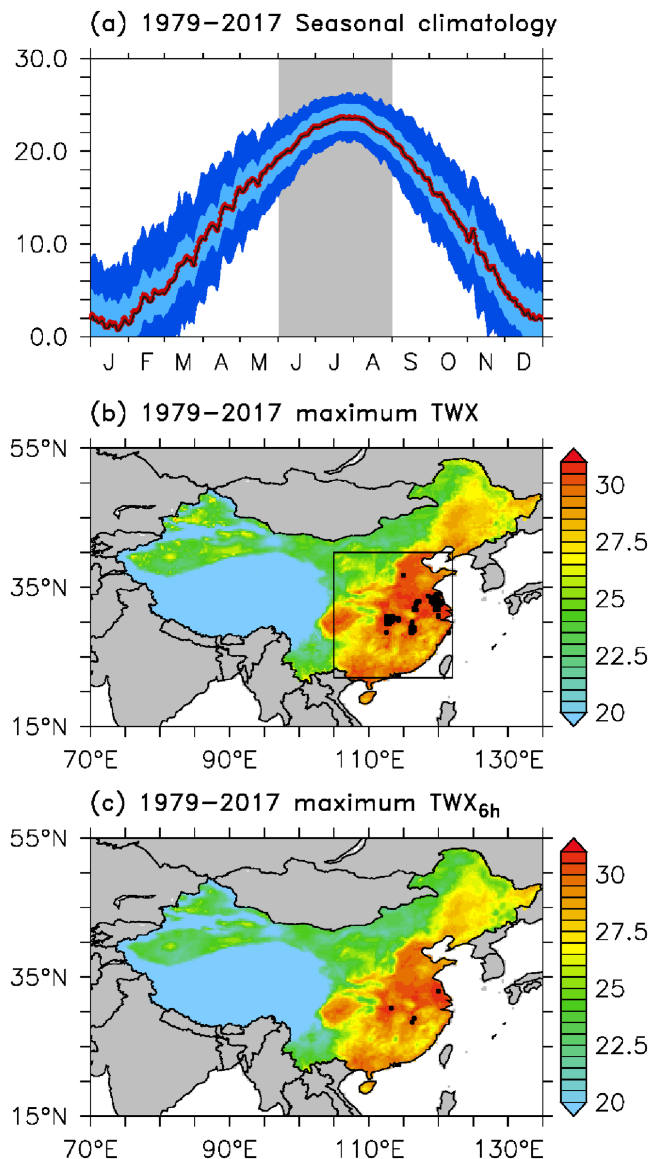
Figure 2. Climatology of wet-bulb temperature and record-breaking events. (a) Southern and Eastern China (105–122°E, 22–40°N, black box in b) daily climatological TWmean (1979–2017) for observations (black solid line) and ERA5 (red solid line). Light blue shading shows the mean ERA5 TW diurnal range, and dark blue shading is the 2.5–97.5% range of TW (based on interannual variability). Gray shading shows JJA. (b) Record-breaking daily maximum ERA5 TWX (from hourly TW) for 1979–2017 period. (c) as (b) but for TWX computed from TW running-mean 6-hr data (TWX_6h) during 1979–2017. In (b) and (c) black dots indicate TW > 31 °C.

of 50 km (Hu et al., 2015) is used to estimate urban trend at each grid point (linearly extended to 2017) and its corresponding effect on T_{mean}. Based on this trend, we then apply an incremental "correction" on daily T_{mean} at each grid point and recompute TW (from daily mean RH and urban corrected T_{mean}). Trends for TW_{mean} with and without urban effect is shown in Figure S4. The effect is weak at regional scale. However, locally difference in trends can reach 0.1 °C per decade, especially around the North China plain. Thus, local TW_{mean} trends could be slightly underestimated in raw data. However, our correction does not include urban effect on RH, which could be opposite sign (drying over urban area) and thus limit T_{mean} amplification. This correction is also difficult to apply at subdaily time scale as it could lead to inconsistent RH and temperature. Thus, this correction is only used as a sensitivity test here. In the main text we use ERA5 without urban correction.

3. Results

3.1. Record-Breaking TW Reaching Dangerous Thresholds

Warm season TW is broadly the same over eastern and southern China (Figure 2a), with the regional mean summer climatology ranging from 20 to 24 °C with a mean diurnal range of 3 °C. Station and reanalysis are broadly consistent for mean TW (Figure S1), confirming the reliability of ERA5 to analyze TW. Although the summer mean is far from critical thresholds, East China is an area with a high daily maximum wet-bulb temperatures (TWX), with record-breaking values around 29 °C during a 6-hr window (based on ERA Interim; Im et al., 2017). Based on hourly data at 0.25° horizontal resolution from ERA5, we found that the highest TWX during the 1979–2017 period was above 31 °C in East China (Figure 2b). These very high wet-bulb temperatures are mainly found in low elevation areas (North China plain and Yangtze river basin) and southern coastal regions, where large cities (such as Shanghai, Chongqing, or Wuhan) are located. At the 6-hr time scale, record-breaking TWX are lower but can still exceed 31 °C locally. We also note that these values may be underestimated due to slightly cold bias in ERA5 compared to observations (Figure S1). This may be partly due to elevation differences between the two data sets, as pointed out in the methodology. As a test, we alternatively corrected RH after 2000 instead of before. Doing so, we found that the critical threshold of 31 °C is exceeded more frequently even at 6-hr time scale (with 6-hr TWX exceedance map being very similar to hourly TWX exceedance map). Estimation of actual TW values in ERA5 is thus sensitive to the reliability of RH. Given the mean differences with OBS over the region (Figure S1c), we estimate the reliability of TW in ERA5 to be about +/−1 °C.

We evaluate processes associated to extreme TW (i.e., the 1% highest daily mean TW_{mean} and daily maximum TWX over the studied region) by performing a composite analysis. The warmest TW events are mainly due to an increase in dry-bulb temperature (Figure 3), occurring when skies are clear (leading to increased solar radiation and net surface shortwaves). Humidity itself does not seem to be a leading factor explaining extreme TW, as RH tends to be stable or decrease slightly. Still, it is noticeable that specific humidity increases during the warmest TW events so RH remains approximately constant and participates in maintaining hot and humid conditions. This behavior is different from European heat waves, which are usually associated with a clear drying (Rebetez et al., 2006).
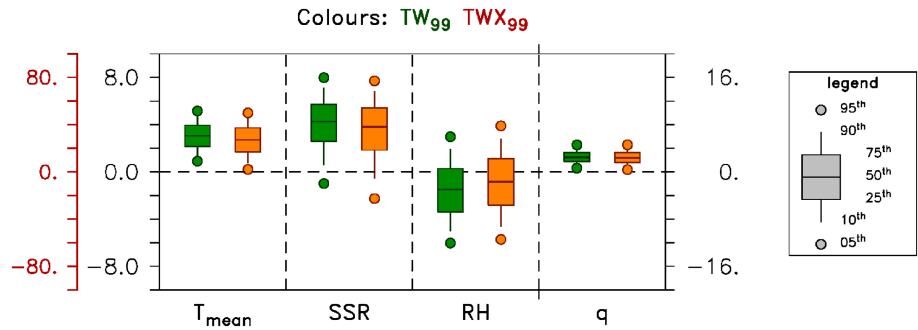
Figure 3. Mechanisms associated to hot extreme wet-bulb temperatures. Composite anomaly of mean dry-bulb temperature (Tmean, °C, black left scale), net shortwave surface radiation (SSR, W/m², red left scale), relative (RH, %, right scale) and specific (q, g/kg, right scale) humidity for extreme TW over southern and eastern China during the 1979–2017 period. Composites are extracted by pooling together anomalies from all grid point and summer days, which are above the 99th percentile values of TW and TWX (TW$_{99}$ and TWX$_{99}$, respectively). All anomalies are relative to the 1979–2017 daily climatology at each grid point.

3.2. Change in Risks During the Last Four Decades

Since 1980 southern China and eastern China have experienced an increase in dry-bulb warm temperature extremes (Figure 4) of about 0.2 °C per decade for the summer means. Wet-bulb temperatures have also warmed although their changes are slightly different compared to dry-bulb temperatures. TW index changes are all fairly consistent with each other while dry-bulb indices show more different behaviors. Dry daily maximum (and summer maximum) increases much faster than daily minimum (and summer minimum). Daily minimum wet-bulb temperatures show a faster increase on average than daily maximum. These differences are clearly translated in terms of diurnal temperature range (DTR) with TW DTR declining of about 0.05 °C per decade while dry-bulb DTR increases by about 0.08 °C per decade (Figure 4). These trends are small but statistically significant and statistically different between wet and dry bulb. This highlights how dry- and wet-bulb temperatures are governed by different processes and how conclusions from dry-bulb temperature studies cannot be directly interpolated to TW. It is also clear that using biased RH data sets leads to drastically underestimating TW trends (illustrated for ERA5 TW$_{mean}$ with the gray box plot in Figure 4). This would result in a trend of less than 0.05 °C per decade (compared to 0.2 °C per decade for corrected data). We have not verify similar computation with ERA Interim, but if RH has similar bias than ERA5, then its implication for TW trends should be the same.

If TWN keeps increasing faster than TWX, it would result in more days with high TW at damaging levels. Long exposure to elevated TW threatens health for vulnerable people and productivity for workers who
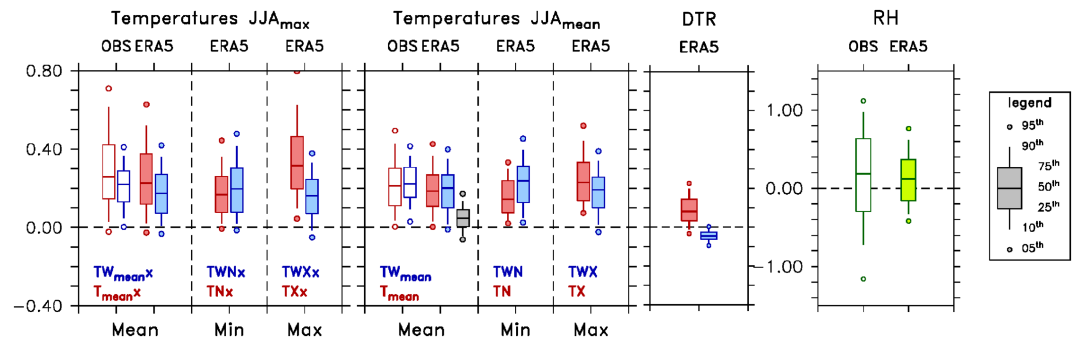

Figure 4. Trends of temperatures and humidity during the 1979–2017 period. Boxplots of trends per decade based on computation at each grid point (over South and East China). Red and blue symbols indicate dry- and wet-bulb temperatures, respectively (°C per decade). Empty symbols are for OBS; filled symbols are for ERA5. Trends are separated for summer maximum (JJA$_{max}$, left) and summer mean (JJA$_{mean}$, middle) values, and for daily mean (TW$_{mean}$ and T$_{mean}$), daily minimum (TWN and TN), and daily maximum (TWX and TX). Trend in JJA$_{mean}$ TW$_{mean}$ for ERA5 without correcting RH is shown by the gray boxplot. Trends in summer mean diurnal temperature range (DTWR, °C per decade) and relative humidity (RH, % per decade) are also displayed.

cannot shelter when outside (such as construction or agricultural workers). Thus, the stability of TW could result in significant threats to Chinese society.

3.3. The Importance of Land Humidity Changes

The above results raise important questions for future projections. If soil moisture is enough to keep RH constant during hot events, then we should expect TW to increase consistently, although slower, with dry-bulb temperatures. Some studies suggest a possible future decrease in RH over land (as indicated by current climate projections under climate warming; Byrne & O'Gorman, 2016). Although this could have a mild moderating effect on TW increase, it is very unlikely to be enough to compensate T increase. For example, a decrease of about 7% in RH would be needed to compensate an increase of 1 °C in T_{mean} and keep TW constant, far from the observed RH reduction (less than 1%/K over China; O'Gorman & Muller, 2010).

One should not forget that dry heat waves are also important. The European 2003 event, which led to thousands of excess deaths (Canoui-Poitrine et al., 2006), was due to dry conditions. Thus, TW is only one of the factors to consider for heat impact projections. Also, future change in land RH is usually estimated in regard to greenhouse gases and other radiative forcing. Other anthropogenic activity could locally modify this response by changing soil water characteristics. This is especially so for agriculture with potentially increased irrigation. Intensified irrigation can create artificial pools of humidity, enhance its availability during warm events, and modify the energy balance. This was already highlighted for the Indus and Ganges valley where irrigation tends to increase TW (Im et al., 2017) and questioned for future projections in the North China plain (Kang & Eltahir, 2018). Changes in vegetation characteristics (and thus evapotranspiration) are also poorly understood. A new generation of climate models with improved land surface processes could change our understanding of future modification in near-surface humidity.

To investigate carefully how TWX would change under climate warming one should use subdaily temperature and humidity data. CMIP5 models already provide surface temperature and humidity outputs at 3-hr time scale. One limitation to understand the full humidity balance between atmosphere and soil is the poor availability of soil moisture data (at daily time scales) in these models. CMIP6 will provide higher frequency outputs for humidity (for both atmosphere and land). This represents valuable sources to understand more clearly how interactions between daily extreme humidity and temperature conditions will evolve in future.

4. Conclusions and Closing Remarks

Characteristics and recent trends of wet-bulb temperatures (TW) in China have been investigated using a new data set of homogenized RH observation to compared with the recent ERA5 reanalysis.

Homogenized observation indicates stable RH during the last four decades, whereas uncorrected observation and reanalysis show a sharp drop in early 2000s, identified as an artifact due to change in measurement methods (stations switching from manual to automatic during this period).

Trend in TW was found to follow closely trends in dry-bulb temperature (T). Although RH has not been identified as a leading factor, humidity supply is an important factor to maintain the same RH level and to allow TW to increase at the same rate as T. Using uncorrected RH data leads to strongly underestimating trends in TW.

Highest TW events were also found to be mainly due to an increase in T, with a stable RH level.

Change in TW for the upcoming decades is still expected to be closely linked to change in T. However, change in RH over land should also play an important role. If RH decrease (drying over land), then it could compensate increase in T and moderate trends in TW. On the other hand, if humidity supply over land is enough to keep RH constant, then TW would keep increasing and could quickly reach dangerous levels. These hypotheses should be investigated using subdaily outputs of land surface moisture from the newly released CMIP6 models.

References

Byrne, M. P., & O'Gorman, P. A. (2016). Understanding decreases in land relative humidity with global warming: Conceptual model and GCM simulations. *Journal of Climate*, *29*, 9045–9061. https://doi.org/10.1175/JCLI-D-16-0351.1

Canoui-Poitrine, F., Cadot, E., & Spira, A. (2006). Excess deaths during the August 2003 heat wave in Paris, France. *Revue d'Épidémiologie et de Santé Publique*, *54*(2), 127–135. https://doi.org/10.1016/s0398-7620(06)76706-2

Davis, R. E., McGregor, G. R., & Enfield, K. B. (2016). Humidity: A review and primer on atmospheric moisture and human health. *Environmental Research*, *144*(Pt A), 106–116. https://doi.org/10.1016/j.envres.2015.10.014

Dee, D. P., Uppala, S. M., Simmons, A. J., Berrisford, P., Poli, P., Kobayashi, S., et al. (2011). The ERA-Interim reanalysis: Configuration and performance of the data assimilation system. *Quarterly Journal of the Royal Meteorological Society*, *137*(656), 553–597. https://doi.org/10.1002/qj.828

Freychet, N., Tett, S., Wang, J., & Hegerl, G. (2017). Summer heat waves over Eastern China: Dynamical processes and trend attribution. *Environmental Research Letters*, *12*(2), 024015.

Freychet, N., Tett, S. F., Hegerl, G. C., & Wang, J. (2018). Central-Eastern China persistent heat waves: Evaluation of the AMIP models. *Journal of Climate*, *31*, 3609–3624. https://doi.org/10.1175/JCLI-D-17-0480.1

Freychet, N., Tett, S. F. B., Bollasina, M., Wang, K. C., & Hegerl, G. C. (2019). The local aerosol emission effect on surface shortwave radiation and temperatures. *Journal of Advances in Modeling Earth Systems*, *11*, 806–817. https://doi.org/10.1029/2018MS001530

Hersbach H., P. de Rosnay, B Bell, D Schepers, A. Simmons, C Soci, et al. (2018). Operational global reanalysis: Progress, future directions and synergies with NWP. European Centre for Medium Range Weather Forecasts. https://doi.org/10.21957/tkic6g3wm

Hu, Y., Jia, G., Pohl, C., Feng, Q., He, Y., Gao, H., et al. (2015). Improved monitoring of urbanization processes in China for regional climate impact assessment. *Environment and Earth Science*, *73*(12), 8387–8404. https://doi.org/10.1007/s12665-014-4000-4

Hutchinson, M. F., McKenney, D. W., Lawrence, K., Pedlar, J. H., Hopkinson, R. F., Milewska, E., & Papadopol, P. (2009). Development and testing of Canada-wide interpolated spatial models of daily minimum-maximum temperature and precipitation for 1961–2003. *Journal of Applied Meteorology and Climatology*, *48*(4), 725–741.

Im, E.-S., Pal, J. S., & Eltahir, E. A. B. (2017). Deadly heat waves projected in the densely populated agricultural regions of South Asia. *Science Advances*, *3*(8).

Kang, S., & Eltahir, E. A. (2018). North China Plain threatened by deadly heatwaves due to climate change and irrigation. *Nature Communications*, *9*(1), 2894. https://doi.org/10.1038/s41467-018-05252-y

Li, Z., & Yan, Z.-W. (2009). Homogenized daily mean/maximum/minimum temperature series for China from 1960-2008. *Atmospheric and Oceanic Science Letters*, *2*(4), 237–243.

Li, Z., Yan, Z.-W., Zhu, Y., Freychet, N., & Tett, S. F. B. (2020). Homogenized daily relative humidity series in China during 1960–2017. *Advances in Atmospheric Sciences*. https://doi.org/10.1007/s00376-020-9180-0

O'Gorman, P. A., & Muller, C. J. (2010). How closely do changes in surface and column water vapor follow Clausius–Clapeyron scaling in climate change simulations? *Environmental Research Letters*, *5*, 025207.

Rebetez, M., Mayer, H., Dupont, O., Schindler, D., Gartner, K., Kropp, J. P., & Menzel, A. (2006). Heat and drought 2003 in Europe: A climate synthesis. *Annals of Forest Science*, *63*(6), 569–577.

Sherwood, S. C., & Huber, M. (2010). An adaptability limit to climate change due to heatstress. *Proceedings of the National Academy of Sciences*, *107*(21), 9552–9555.

Stull, R. (2011). Wet-Bulb temperature from relative humidity and air temperature. *Journal of Applied Meteorology and Climatology*, *50*, 2267–2269.

Wang, J., Tett, S. F. B., & Yan, Z. (2017). Correcting urban bias in large-scale temperature records in China, 1980–2009. *Geophysical Research Letters*, *44*(1), 401–408. https://doi.org/10.1002/2016GL071524

Willett, K. M., Dunn, R. J. H., Thorne, P. W., Bell, S., de Podesta, M., Parker, D. E., et al. (2014). HadISDH land surface multi-variable humidity and temperature record for climate monitoring. *Climate of the Past*, *10*(6), 1983–2006. https://doi.org/10.5194/cp-10-1983-2014

Willett, K. M., Jones, P. D., Gillett, N. P., & Thorne, P. W. (2008). Recent changes in surface humidity: Development of the HadCRUH dataset. *Journal of Climate*, *21*(20), 5364–5383.

Yu, J., & Mou, R. (2008). Research on the cause of difference between AWS- and MAN-Relative humidity observations. *Meteorological Monographs* (in Chinese), *34*(12), 96–102.

Yuan, Y., Zhao, X. L., Wang, X. L., & You, Y. (2010). The difference of the relative humidity between automatic and manual observations. *Meteorological Monographs* (in Chinese), *36*(2), 102–108.

Zhu, Y. N., Cao, L. J., Tang, G. L., & Zijiang, Z. (2015). Homogenization of surface relative humidity over China. *Advances in Climate Change Research* (in Chinese), *11*(6), 379–386. https://doi.org/10.3969/j.issn.1673-1719.2015.06.001